3D Multifields FEM Computation of Transverse Flux Induction Heating for Moving-Strips

Z. Wang W. Huang W. Jia Q. Zhao Y. Wang W. Yan
Hebei University of Technology, 300130 Tianjin, China
D. Schulze G. Martin U. Luedtke
Technical University of Ilmenau, 98684 Ilmenau, Germany

Abstract - **The numerical and experimental studies on induction heating of continuously moving strips in transverse field are presented in this paper. The induced eddy current and its coupled thermal field in moving media is computed with FEM. The adopted mathematical model consists of a Fouriers thermal conduction equation and a set of differential equations, which describes the steady-state eddy current problem in a configuration comprising a magnetic vector potential and an electrical scalar potential. The calculated results are in good agreement with the measurement.**

Index Terms- **Transverse flux, FEM computation, Induction heating, Eddy current, temperature field, 3D, Moving object**

I. Introduction

Induction heating processes for heating plates and strips provide significant technological, economic and ecological advantages in comparison with conventional oil- or gas-fired plants: fast heating rate, instant controllability, high efficient and minimal environment pollution. Because of skin effect the induction heating in a longitudinal flux is limited only for electric thick plate. The limits are lifted by the transverse flux induction heating(TFIH). In TFIH the eddy currents induced in the workpiece close within the workpiece surface. The frequency used here must be matched to the size of the workpiece if power is to be transferred efficiently from the induction coil. To achieve a completely uniform temperature across the entire strip width is consequently a critical factor

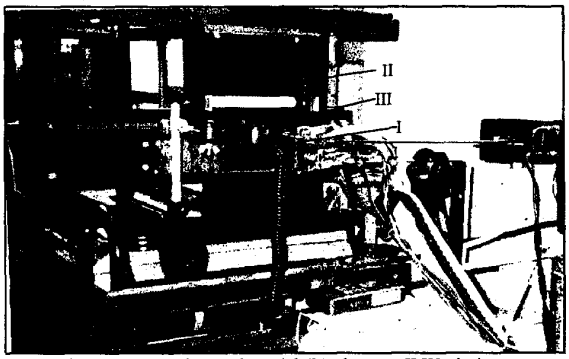

Fig. 1. Experimental model (I Inductor ; II Workpiece; III Measurement instrument)

Manuscript received on June 1, 1998.
Z. Wang. Tel/fax +86-22-26545277, zmwang@hebut.edu.cn.
This project is supported in part by the CEC and HBSTC, China

in the development of a practical TFIH. The design of the TFIH equipment necessitates accurate process performance prediction for the thermal characteristic particularly in large scale equipment with more than several MW power energy consuming. This simulation is only possible with 3D eddy current computation coupled with thermal and mechanical force field. A 3d FEM multi-field simulation is used for developing such equipment.

II. Mathematical Model

The problem considered here is that of eddy current at low angular frequency ω. The displacement currents are ignored. magnetic permeability μ and electric conductivity κ are assumed to be constant over a long period. The mathematical model for this sinusoidal quasi-static eddy current problem results from the Maxwell equations and the complex magnetic vector potential $\underline{\vec{A}}$ and a complex scalar potential $\underline{\phi}$

$$\text{rot}\left(\frac{1}{\mu}\text{rot}\,\underline{\vec{A}}\right)-\vec{v}\times\nabla\times\underline{\vec{A}}+j\omega\kappa\left(\underline{\vec{A}}-\text{grad}\,\underline{\phi}\right)=\kappa\,\underline{\vec{E}}_0 \quad (1)$$

$$div(\vec{v}\times\nabla\times\underline{\vec{A}}-j\omega\kappa\underline{\vec{A}}+\omega\kappa\ grad\ \underline{\phi})=0 \quad (2)$$

$\underline{\vec{E}}_0$ is the electric field field strength impressed by the power source.

The eddy current density is computed as follows,

$$\underline{\vec{J}}=\vec{v}\times\nabla\times\underline{\vec{A}}-j\omega\kappa\underline{\vec{A}}+\omega\kappa\ grad\ \underline{\phi}+\kappa\underline{\vec{E}}_0 \quad (3)$$

The influence of the movement of strip to the magnetic field distribution(by velocity $\vec{v}$ >1.0 m/s) is very small and can be neglected.

The current density determines the heat source distribution:

$$p_v=\frac{|\underline{J}|^2}{\kappa} \quad (4)$$

The temperature field $\vartheta(x,y,z)$ is computed based on the Fourier's thermal conduction equation,

$$\frac{\partial(c,\rho,\vartheta)}{\partial t}=\text{div}\left(\lambda\ \text{grad}\,\vartheta\right)+p_V-\vec{v}\,grad(c,\rho,\vartheta) \quad (5)$$

where λ is the thermal conductivity coefficient, c is the specific heat, ρ is the mass density and $\vec{v}$ is the strip

velocity. The coefficient λ and c are dependent on the temperature.

The two field, the electromagnetic field and temperature field, which becomes steady-state at the constant velocity, are coupled via the dependence of temperature of the electrical conductivity and the magnetic permeability. By the practical computation a compromise has been made between the exact wished and the time saving computation.

Forces which can be calculated using the computed field variables $\vec{A}$ and $\vec{J}$ act through the electromagnetic field on the strip. Only the Lorentz force acts on a non-ferromagnetic workpiece. The force $\vec{F}_v$ related to the unit of volume can be split into a mean value and a portion oscillating at twice the inductor current frequency.

$$\vec{F}_v = \mathrm{Re}\left\{\vec{J} \times \left(\mathrm{rot}\,\underline{\vec{A}}\right)^*\right\} + \left(\vec{J} \times \mathrm{rot}\,\vec{A}\right)\cos\left(2\omega t\right) \qquad (6)$$

In the case of ferromagnetic workpieces, interfacial forces $\vec{F}_A$ are also effective. Assuming that the permeability of the workpiece μ is much greater than that of air μ_0 $(\mu >> \mu_o)$,

$$\vec{F}_A = \frac{\vec{n}}{2}\left(\frac{1}{\mu_o}\left(rot\ \vec{A}\right)_n^2 + \frac{1}{\mu}\left(rot\ \vec{A}\right)_t^2\right)\left(1+\cos\left(2\omega t\right)\right) \qquad (7)$$

III. Boundary Conditions

The computation of the electromagnetic field by approximation is performed on the basis of the finite element method. The Galerkin method is applied to the differential equations (1) and (2). An illustratively model of the designed finite element mesh is shown in fig. 2. In order to decrease the computation time, the real investigations were made with a quarter of this mesh. If you look at fig. 2, you can easily find two additional planes of symmetry, situated in the middle of the strip (x-y plane) and in the middle of the inductor-yoke

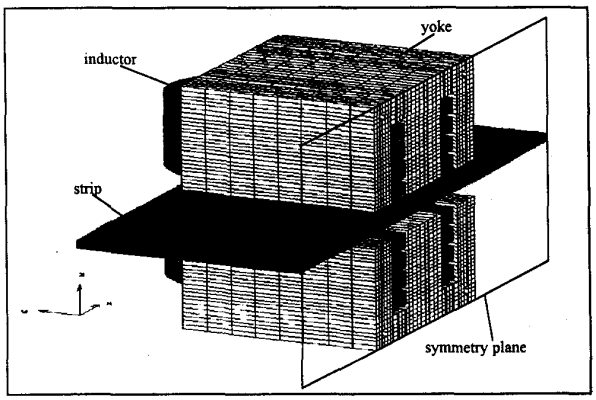

Fig.2. Inductor of the TFIH equipment with meshes

combination(y-z plane). By using of the given boundary and symmetrical boundary conditions, we can work with this quarter part.

The related boundary and symmetry conditions are considered. In the x-z and the y-z symmetric planes, the electric current density is oriented perpendicular to these planes. Hence the tangential components of the magnetic vector potential $\underline{\vec{A}}$ and the scalar potential $\underline{\varphi}$ are:

on the x-z plane:

$$\underline{\vec{A}}_x = \underline{\vec{A}}_z = 0 \qquad (8)$$

$$\frac{\partial \underline{\vec{A}}_y}{\partial y} = 0 \qquad (9)$$

$$\underline{\varphi} = 0 \qquad (10)$$

and on the y-z plane

$$\underline{\vec{A}}_y = \underline{\vec{A}}_z = 0 \qquad (11)$$

$$\frac{\partial \underline{\vec{A}}_x}{\partial x} = 0 \qquad (12)$$

$$\underline{\varphi} = 0 \qquad (13)$$

On the x-y symmetrical plane, the current density has no perpendicular component, hence

$$\underline{\vec{A}}_z = 0 \qquad (14)$$

$$\frac{\partial \underline{\vec{A}}_x}{\partial x} = \frac{\partial \underline{\vec{A}}_y}{\partial y} = 0 \qquad (15)$$

$$\frac{\partial \underline{\varphi}}{\partial z} = 0 \qquad (16)$$

The present problem has an open boundary condition because the vector potential disappears only in the infinity. With the aids of comparative computations, an enveloping surface can, however, be determined for which the condition

$$\underline{\vec{A}} = 0 \qquad (17)$$

is valid within a defined upper limit of error.

The temperature field must only be computed for the workpiece. The boundary condition on the entering side of the strip is

$$\vartheta(x,y,z)\big|_{\Gamma_1} = \vartheta_0(x,y,z)\big|_{\Gamma_1} \qquad (18)$$

where ϑ_0 is the ambient temperature. Because of the mass-bound heat transfer in the direction of the velocity $\vec{v}$, there is no y-z symmetric plane. The heat source density in newly added area can be obtained by reflection at the y-z plane or by separated computation for a corresponding temperature distribution. Thermal losses by convection and radiation on the strip surface are also considered.

The boundary condition on the strip surface is:

$$-\lambda\frac{\partial \vartheta}{\partial n} = \alpha_k(\vartheta - \vartheta_U) + \alpha_s(\vartheta - \vartheta_U)\big|_{\Gamma_3} \qquad (19)$$

On the exit side

$$\frac{\partial \vartheta}{\partial x} = 0 \qquad (20)$$

is indicated.

Thermal losses by convection and radiation on the strip surface are considered with the Cauchy boundary condition.

$$\lambda\, grad\vartheta \cdot \vec{n} = \alpha(\vartheta_0 - \vartheta) \qquad (21)$$

where α is the heat transfer-coefficient for convection and radiation, and ϑ_0 the ambient temperature respectively. Therefore the computation of the temperature field of the moving strip could be done advantageously on the basis of particular grid. The distribution of heat sources, in form of node values, is transferred to this new grid from the old grid by means of the shape functions. The influence of the velocity destroys the coefficient matrix symmetry of the equation system. Test computation reveals that a better stability is obtained by transient computation, wherefore the Crank-Nickelson method is applied. Convergence problems at an increasing velocity are eliminated by adopting shorter time steps.

IV. RESULTS

The numerical method presented here was verified by measurements on an experiment installation for homogenous preheating/reheating of strips [2],[4]. The inductors of this installation are arranged according to Fig. 1. The calculated eddy current distribution on the strip surface is illustrated in Fig. 3. Because the depth of current penetration is much greater than the strip width, a similar eddy current distribution will also occur in the deeper layers.

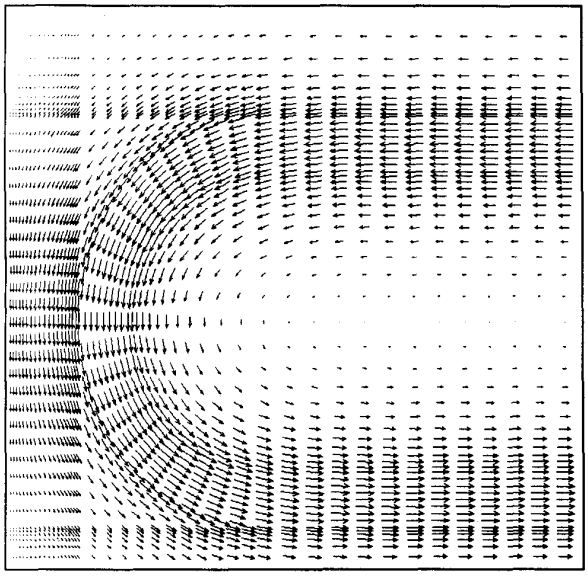

Fig. 3 Eddy current distribution on the strip surface (half)

The TFIH is widely used to make a uniform temperature distribution by the continuously strip heating. The long side of the inductor protruding beyond the strip edge lead to overheating. The short side of the inductor result in a temperature decrease. Joint application of both effects results in a multitude of feasible combinations going from extreme edge overheating to undercooling. With an optimised design, they can also result in almost homogenous temperature distribution across the strip width.

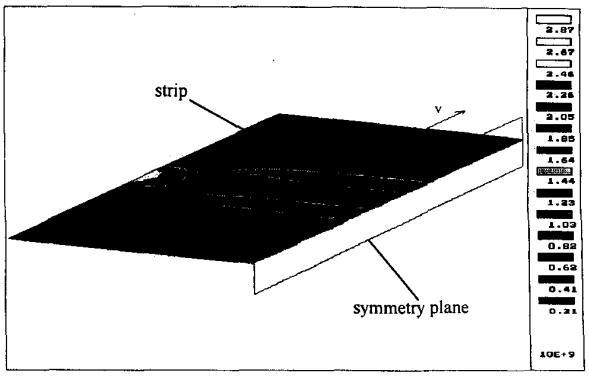

Fig. 4. Distribution of heat source density in the workpiece.

Fig. 5 shows the temperature distribution resulting from the reflected heat sources distribution as per Fig. 4 in the steady-state situation. The computed results are confirmed by temperature measurements performed with an infrared camera shown in Fig. 6.

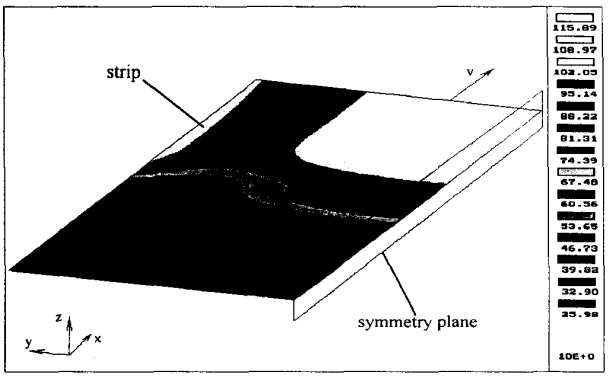

Fig. 5. Steady-state temperature distribution on the strip surface

The presented accurate numerical model permits finding an optimal design by variation without having to perform high-cost time-consuming experiments. The design sought can, for instance, be the one which, at a specified distance "a" (Fig. 1) from the last inductor, results in a temperature distribution $\vartheta(y,z)$ with the restriction

$$\vartheta_{\min} < \vartheta(y,z)\big|_{x=a} < \vartheta_{\max} \qquad (22)$$

If further latitude for variation remains on fulfilment of this requirement, the task of optimisation can be extended to include low energy consumption or a high over efficiency

$$\eta = \eta_{in} \cdot \eta_{el} \cdot \eta_{th} \rightarrow \max \qquad (23)$$

The efficiency of frequency converter, resonant circuit and supply conductors η_{in} is generally independent of the TFIH inductor design. However, the product of the electric and thermal efficiencies $\eta_{e\ell} \cdot \eta_{th}$ essentially depends on the design.

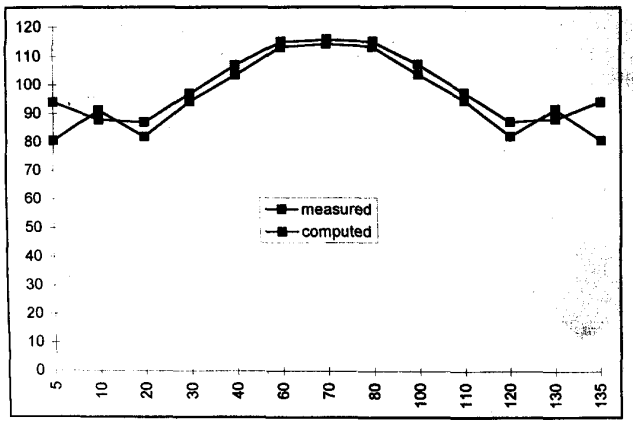

Fig. 6. Temperature distribution across the stripwidth at the outlet side

The computed results shown on the laboratory model are confirmed by temperature measurements in fig. 6. The close agreement verifies the accuracy of the models above.

V. CONCLUSION

Induction heating found more and more application in the metallurgy industry. Electromagnetic processing of materials can brings new world not only for new technology, but also for new materials. The simulation is necessary and possible with 3D eddy current computation coupled with thermal and mechanical force field.

REFERENCES

[1] O. Biro; K. Preis, "On the use of the magnetic vector potential in the finite element analysis of three-dimensional eddy currents", *IEEE Transactions on Magnetics*, vol. 25, no. 4, pp. 3145-3159, July 1989.

[2] D. Schulze Z. Wang, B. Nacke, "Developing an universal TFIH equipment using 3d eddy current field computation ", *IEEE Trans. on Mag*, vol. 32, no.3, pp.1609-1612, May 1996

[3] Z. Wang, "Modellierung und optimaler Entwurf der Querfelderwaermung", PhD Dissertation, TU Ilmenau, 1996.

[4] W. Andree, D. Schulze, Z. Wang, "3D FEM Eddy current computation in the transverse flux induction heating equipment" *IEEE Trans. on MAG*, vol 30, No. 4, 1994